

Bose polarons as relativistic Unruh-DeWitt detectors: Entanglement harvesting from Bose-Einstein condensates

T. Rick Perche,^{1,*} Francesco Gozzini,^{2,†} and Markus K. Oberthaler^{2,‡}

¹*Nordita, KTH Royal Institute of Technology and Stockholm University,
Hannes Alfvéns väg 12, 23, SE-106 91 Stockholm, Sweden*

²*Kirchhoff-Institut für Physik, Universität Heidelberg,
Im Neuenheimer Feld 227, 69120 Heidelberg, Germany*

We show that a bound impurity in a Bose-Einstein condensate can be directly mapped to an Unruh-DeWitt detector interacting with a relativistic quantum field. We provide explicit experimental parameters for an implementation using ^{39}K impurities coupled to a ^{87}Rb condensate via finite-time Feshbach tuning. As an application, we study the extraction of vacuum entanglement from distant regions of the condensate and find viable parameters for the implementation of entanglement harvesting.

Introduction—The advent of quantum field simulators capable of reproducing aspects of quantum field dynamics in curved spacetime has created unprecedented opportunities to test foundational predictions of relativistic quantum field theory (QFT) [1–3]. A growing number of analog platforms — ranging from ultracold atoms and trapped ions [4] to photonic [5] and superconducting architectures [6] — can engineer effective metrics, horizons, and nontrivial expansion dynamics [7]. As a result, phenomena long viewed as purely theoretical, such as horizon-induced correlations [8], particle production in time-dependent backgrounds [1, 9], and entropy measurements in QFT [10], are becoming experimentally accessible. These new experimental capabilities open a path toward using laboratory systems to probe regimes that lie far beyond the reach of astrophysical or cosmological measurements.

The key feature of all experimental systems so far is the ability to directly detect spatial correlations of the analog relativistic quantum field. However, we are still missing implementations of probes that can couple to the field locally in space and time. Local measurements are essential for probing fundamental features of QFTs that only become evident in finite spacetime regions, such as properties of local algebras [11, 12], covariant measurement schemes [13, 14], and more relevant for this work, entanglement between non-complementary regions [15–17].

Local probes in QFT are usually implemented as particle detector models, or Unruh-DeWitt (UDW) detectors [18–20]. These consist of effectively any localized quantum system that couples to a quantum field [21, 22]. For instance, UDW detectors can be implemented in practice with electro-optic sampling [23, 24], superconducting qubits [25], and proposals for interferometric schemes in Bose-Einstein condensates have been put forward [26, 27]. When coupled for finite times, UDW de-

tectors can implement quantum information protocols that fully utilize the local degrees of freedom of quantum fields [28–30]. In particular, they can quantify entanglement in the vacuum of a relativistic QFT through entanglement harvesting [31–34]. In the protocol, yet to be implemented experimentally, entanglement is extracted from the quantum field by causally disconnected probes.

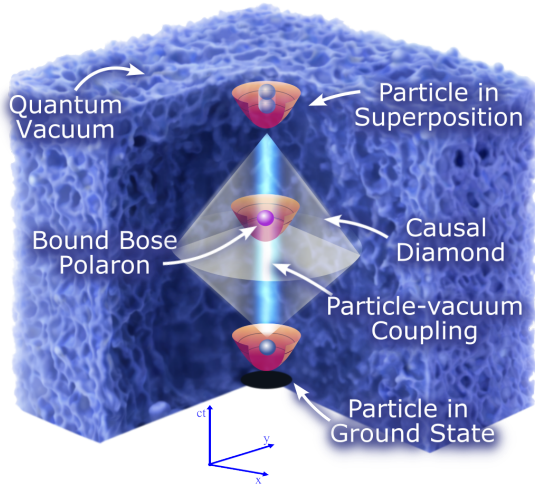


Figure 1. A bound Bose polaron as an Unruh-DeWitt detector. An impurity trapped in a harmonic trap is coupled for a finite time with a Bose-Einstein condensate (BEC) by temporal Feshbach tuning to non-vanishing scattering length. The detector probes local degrees of freedom of the condensate in a causal diamond, determined by the speed of sound. After the interaction, the impurity is partially in a superposition of motional ground and excited state, revealing quantum information of the quantum state of the BEC.

Here, we show that a bound Bose polaron —a trapped impurity immersed in a Bose-Einstein condensate (BEC) [35, 36] —realizes a microscopic implementation of an Unruh-DeWitt detector coupled to the effective relativistic phonon field of the condensate. Ultracold gases offer pristine control over motional degrees of freedom, i.e., spatial mode structure of the detector, as well as inde-

* rick.perche@su.se

† gozzini@thphys.uni-heidelberg.de

‡ markus.oberthaler@kip.uni-heidelberg.de

pendent temporal control of the impurity–phonon coupling. This realizes a spatiotemporally localized detector suitable for probing quantum-information–theoretic phenomena such as entanglement harvesting. Our microscopic derivation expresses the detector gap, coupling strength, and switching function in terms of experimentally controllable parameters, providing concrete prescriptions for implementing relativistic detector physics in current ultracold atom setups.

Local probes in QFT—The degrees of freedom of a relativistic quantum field theory are spread over space-time regions that are fully determined by information at a given surface, the so-called causal diamonds [37–39]. Due to this fact, long-time interactions effectively probe degrees of freedom localized in a spatial region with extension much larger than the probe itself. Local effects in QFT can then only be seen when probing the field for finite times [40], for instance using UDW detectors.

In its simplest form, a UDW detector consists of a two-level system linearly coupled to a free scalar quantum field $\hat{\phi}(\mathbf{x})$ in a background spacetime \mathcal{M} . However, here we focus on the case where the detector couples to the conjugate momentum $\hat{\pi}(\mathbf{x}) = \partial_t \hat{\phi}(\mathbf{x})$ in 3+1 dimensional Minkowski spacetime [41–43] with inertial coordinates $\mathbf{x} = (t, \mathbf{x})$. We also assume that the probe undergoes an inertial trajectory. If the energy gap between the detector’s ground and excited states is Ω , the coupling between the probe and the field $\hat{\pi}(\mathbf{x})$ is described by an interaction Hamiltonian density of the form [44]

$$\hat{\mathcal{H}}_I(\mathbf{x}) = \lambda(\Lambda^*(\mathbf{x})e^{i\Omega t}\hat{\sigma}^+ + \Lambda(\mathbf{x})e^{-i\Omega t}\hat{\sigma}^-)\hat{\pi}(\mathbf{x}), \quad (1)$$

where λ is a coupling constant, $\Lambda(\mathbf{x}) = \chi(t)f(\mathbf{x})$ is a spacetime smearing function that factors as a (dimensionless) real switching function $\chi(t)$ and a (potentially complex) smearing function $f(\mathbf{x})$ with units of density. $\Lambda(\mathbf{x})$ determines the region of spacetime in which the probe couples to the field, and $e^{\pm i\Omega t}\hat{\sigma}^\pm$ are the time-evolved raising and lowering operators in the detector Hilbert space. We use conventions such that $\hat{\pi}^2$ has units of energy density.

Applications of the UDW model in curved spacetimes and non-inertial trajectories have been proven effective for studying effects such as Hawking radiation [45–47] and the Unruh effect [18, 48–51]. Moreover, the UDW model has been shown to reproduce the essential features of the interactions of quantum fields coupled to any bosonic field, such as an atom or superconducting qubits coupled to electromagnetism [52–54], and quantum systems coupled to linearized quantum gravity [55–57]. However, the difficulties in implementing a finite-time coupling present a significant challenge to the experimental implementation of UDW detectors [58].

A two-level system that interacts with the field according to Eq. (1) samples field degrees of freedom localized within the causal diamond that contains the region where $\Lambda(\mathbf{x})$ is non-zero, allowing direct access to local observables in QFT [13]. Indeed, to leading order in the cou-

pling constant λ , the detector’s final state only depends on the two-point function of $\hat{\pi}(\mathbf{x})$ smeared against the region $\Lambda(\mathbf{x})$. Explicitly, the vacuum two-point function of the operator $\hat{\pi}(\mathbf{x})$ can be written as

$$\langle \hat{\pi}(\mathbf{x})\hat{\pi}(\mathbf{x}') \rangle = \frac{1}{(2\pi)^3} \int d^3\mathbf{k} \frac{\hbar\omega_{\mathbf{k}}}{2} e^{i\mathbf{k}\cdot(\mathbf{x}-\mathbf{x}')}, \quad (2)$$

where $\mathbf{k}\cdot\mathbf{x} = -\omega_{\mathbf{k}}t + \mathbf{k}\cdot\mathbf{x}$, $\omega_{\mathbf{k}} = c|\mathbf{k}|$, and c is the speed of light. The final state of a UDW detector only depends on the two-point function (2) integrated along the support of $\Lambda(\mathbf{x})$.

Phonons as relativistic quantum field—Since the seminal paper by Unruh on experimental black hole evaporation [59], numerous theoretical and experimental results building on the analogy between propagation of fields in curved spacetimes and propagation of sound waves in fluids have been obtained [7]. Especially, atomic superfluids are an ideal platform to implement quantum field simulators, as low-energy phonons behave as a quantum massless scalar field in a Lorentzian metric determined by the background condensate [60, 61]. By splitting the atomic quantum field as a classical background and quantum fluctuations, $\hat{\Psi}(\mathbf{x}) = \Psi_0(\mathbf{x}) + \delta\hat{\Psi}(\mathbf{x})$ [62], the BEC density can be written (to leading order in the fluctuations) as

$$\hat{\rho}_b(\mathbf{x}) = \hat{\Psi}^\dagger(\mathbf{x})\hat{\Psi}(\mathbf{x}) \approx \rho_0(\mathbf{x}) + \delta\hat{\rho}(\mathbf{x}). \quad (3)$$

Here, $\rho_0 = \Psi_0^\dagger \Psi_0$ is the (classical) background density and $\delta\hat{\rho}(\mathbf{x})$ encodes its quantum fluctuations. It can be shown that in the low-energy regime $\delta\hat{\rho}$ behaves analogously to the momentum of a real scalar field (see e.g. [63] and Appendix A). This quantum field evolves in a spacetime with Lorentzian metric where the effective speed of light is given by the speed of sound in the BEC. The speed of sound in the condensate is given by $c_s^2 = \rho_0 g_{bb}/m_b$, where $g_{bb} = 4\pi\hbar^2 a_{bb}/m_b$; here a_{bb} is the s -wave scattering length characterizing the boson–boson interaction and m_b is the mass of the boson. In particular, when the density of the condensate is constant $\rho_0(\mathbf{x}) = \rho_0$, i.e., $c_s(\mathbf{x}) = c_s$ and the effective spacetime is Minkowski. The density fluctuations $\delta\hat{\rho}(\mathbf{x})$ can then be written as

$$\delta\hat{\rho}(\mathbf{x}) = \frac{1}{\sqrt{g_{bb}V}} \sum_{\mathbf{k} \neq 0} \sqrt{\frac{\hbar\omega_{\mathbf{k}}}{2}} \left(\hat{b}_{\mathbf{k}} e^{i\mathbf{k}\cdot\mathbf{x}} + \hat{b}_{\mathbf{k}}^\dagger e^{-i\mathbf{k}\cdot\mathbf{x}} \right), \quad (4)$$

with V the normalization volume, $\hat{b}_{\mathbf{k}}, \hat{b}_{\mathbf{k}}^\dagger$ the phonon creation and annihilation operators, $\mathbf{k}\cdot\mathbf{x} = -\omega_{\mathbf{k}}t + \mathbf{k}\cdot\mathbf{x}$, and we assume the relativistic dispersion (energy-momentum) relation $\omega_{\mathbf{k}} \approx c_s|\mathbf{k}|$, which holds in the low energy regime. Notice that the two-point function of the density fluctuations can then be written as

$$\langle \delta\hat{\rho}(\mathbf{x})\delta\hat{\rho}(\mathbf{x}') \rangle = \frac{1}{g_{bb}V} \sum_{\mathbf{k} \neq 0} \frac{\hbar\omega_{\mathbf{k}}}{2} e^{i\mathbf{k}\cdot(\mathbf{x}-\mathbf{x}')}, \quad (5)$$

analogous to the two-point function of the conjugate momentum operator in Eq. (2) in a finite volume [64], with the additional factor of g_{bb}^{-1} .

Impurities as local probes— Immersing a distinguishable particle, typically of a different atomic species, in Bose-Einstein condensates has been studied in detail and is connected to the physics of polarons in solid state physics [36]. Here, we will use the additional control to trap the impurity in a harmonic trap realized with a species-dependent light-shift potential giving rise to a bound Bose polaron. This has already been studied experimentally with a mixture of lithium (impurity) and sodium (BEC), revealing decoherence of motional degrees of freedom [65] and the analog of the Lamb shift due to the coupling to the phononic quantum field [66]. In the weakly interacting limit, which is the regime we are exploiting here, the Bose polaron is known as the Fröhlich polaron [67–69]. Effectively, the impurity interaction with the BEC is a density-density coupling, controlled by the parameter $g_{ab} = 2\pi\hbar^2 a_{ab}/\mu_{ab}$. Here $\mu_{ab} = m_a m_b / (m_a + m_b)$ is the reduced mass, m_a is the mass of the impurity atom, and a_{ab} is the interspecies s-wave scattering length. Explicitly, we can write the interaction Hamiltonian density (in the interaction picture) as

$$\hat{\mathcal{H}}_I(\mathbf{x}) = g_{ab} \hat{\rho}_a(\mathbf{x}) \hat{\rho}_b(\mathbf{x}), \quad (6)$$

where $\hat{\rho}_a(\mathbf{x})$ is the time-evolved density of the impurity. Denoting the localized eigenstate of the impurity atom with energy Ω_n by $|\mathbf{n}\rangle$ and their wavefunctions by $\psi_{\mathbf{n}}(\mathbf{x}) = \langle \mathbf{x} | \mathbf{n} \rangle$, we can write

$$\hat{\rho}_a(\mathbf{x}) = \sum_{\mathbf{n}\mathbf{m}} \psi_{\mathbf{n}}^*(\mathbf{x}) \psi_{\mathbf{m}}(\mathbf{x}) e^{i(\Omega_n - \Omega_m)t} |\mathbf{n}\rangle \langle \mathbf{m}|. \quad (7)$$

From now on we assume that the only relevant energy levels in Eq. (7) are its ground (g) and excited (e) states. The two-level impurity field operator then becomes

$$\begin{aligned} \hat{\rho}_a(\mathbf{x}) = & e^{i\Omega t} (\psi_e^* \psi_g)(\mathbf{x}) \hat{\sigma}^+ + e^{-i\Omega t} (\psi_g^* \psi_e)(\mathbf{x}) \hat{\sigma}^- \\ & + |\psi_e(\mathbf{x})|^2 \hat{\sigma}^+ \hat{\sigma}^- + |\psi_g(\mathbf{x})|^2 \hat{\sigma}^- \hat{\sigma}^+ \end{aligned} \quad (8)$$

where $\Omega = \Omega_e - \Omega_g$ and $\hat{\sigma}^\pm$ are the raising and lowering operators between the states $|g\rangle$ and $|e\rangle$. Since the last two diagonal terms in (8) are projectors and do not contribute to the excitation probability of the impurity [19], we drop them in the following. Analogously, in (6) we can replace $\hat{\rho}_b(\mathbf{x})$ with $\delta\hat{\rho}(\mathbf{x})$, as ρ_0 is a classical term proportional to the identity. Remarkably, the polaron model also allows for a time-varying coupling $g_{ab}(t)$ to be implemented, allowing one to write the interaction Hamiltonian as

$$\hat{\mathcal{H}}_I(\mathbf{x}) = \bar{g}_{ab} \chi(t) (f^*(\mathbf{x}) e^{i\Omega t} \hat{\sigma}^+ + f(\mathbf{x}) e^{-i\Omega t} \hat{\sigma}^-) \delta\hat{\rho}(\mathbf{x}), \quad (9)$$

where $f(\mathbf{x}) = (\psi_g^* \psi_e)(\mathbf{x})$ and we write $g_{ab}(t) = \bar{g}_{ab} \chi(t)$, factoring out the time dependence in a dimensionless

switching function $-1 \leq \chi(t) \leq 1$. Comparing (9) with (1) shows that the polaron is effectively a UDW detector for the phonon density field. Introducing a timescale T that controls the switching of the interaction through $\chi(t) = \beta(t/T)$, the momentum-coupled UDW detector can be mapped to the polaron model by

$$\hat{\pi}(\mathbf{x}) \mapsto \sqrt{\frac{c_s}{c}} \sqrt{g_{bb}} \delta\hat{\rho}(\mathbf{x}), \quad \lambda \mapsto \sqrt{\frac{c}{c_s}} \frac{\bar{g}_{ab}}{\sqrt{g_{bb}}}, \quad (10)$$

and the relevant rescalings $\Omega \mapsto \frac{c_s}{c} \Omega$ and $T \mapsto \frac{c_s}{c} T$.

Arguably, the most important feature of an UDW detector is to allow finite-time coupling with the field. The control of $g_{ab}(t)$ is achieved by magnetically tuned Feshbach resonances [70]. Most distinct pairs of atomic species allow a value of the magnetic field B_0 such that scattering length $a_{ab}(B_0) = 0$, implying $g_{ab} = 0$, thus decoupling the impurity and the BEC. Applying a magnetic pulse to the system by varying the external magnetic field $B(t)$ away from B_0 , we can implement a finite time coupling, in perfect analogy with the detector model in Eq. (1).

We can explicitly see how the impurity can measure localized field observables through a finite-time interaction by noticing that its vacuum excitation probability (see Appendix B) is given by

$$\mathcal{L} = \frac{\bar{g}_{ab}^2}{\hbar^2} \langle \delta\hat{\rho}(\Lambda^-) \delta\hat{\rho}(\Lambda^+) \rangle, \quad (11)$$

where $\delta\hat{\rho}(\Lambda^\pm) \equiv \int d^4x \Lambda^\pm(\mathbf{x}) \delta\hat{\rho}(\mathbf{x})$ are the smeared field observable localized by the spacetime functions $\Lambda^-(\mathbf{x}) = \chi(t) f(\mathbf{x}) e^{-i\Omega t}$ and $\Lambda^+(\mathbf{x}) = \Lambda^-(\mathbf{x})^*$. The shape of the wavefunction $(\psi_g^* \psi_e)(\mathbf{x})$ determines the spatial localization of the observables probed, and $\chi(t)$ their extension in time, encoding expected values of local operators of algebraic QFT in directly accessible physical quantities.

Experimental implementation—The experimental system of ultracold mixtures offers a broad range of control parameters, which we will discuss in the context of UDW detectors and relativistic quantum fields. As a very suitable combination of species, we propose a potassium–rubidium mixture [71], where species-selective trapping of ^{39}K in a light-shift potential realizes the trapped impurity, while ^{87}Rb acts as the substrate for the phononic relativistic quantum field [72]. The large fine-structure splitting of rubidium allows for the realization of dipole potentials utilizing the existence of a tune-out wavelength [73], i.e., the light-shift potential is only seen by potassium atoms. The trap frequencies can be tuned from a few hundred hertz to several tens of kilohertz.

Additionally, the s-wave scattering length for rubidium is $a_{bb} \sim 100 a_0$, where a_0 is the Bohr radius, combined with the low three-body loss rates, allows for the preparation of large and high-density Bose–Einstein condensates in two and three spatial dimensions [74, 75]. For the reported peak density $\rho_0 \sim 5 \times 10^{14} \text{ atoms cm}^{-3}$, the

speed of sound is $c_s \sim 4.4$ mm/s and the healing length is $\xi \sim 120$ nm. Length scales larger than ξ are well captured by the relativistic (phononic) approximation.

The interaction between rubidium and potassium can be controlled via Feshbach resonances employing controlled magnetic fields [76]. For our purposes, the zero crossing of the interaction, i.e., decoupling the detector from the relativistic scalar field, is important and has been studied in detail in the past [77, 78]. Additionally, the interaction can be changed by small variations of the magnetic field (~ 1 G) to values as high as $a_{ab} = 1000 a_0$, without significant loss during the short coupling time of \sim ms [79]. The scattering properties of rubidium are not changed when varying the magnetic field in this range, ensuring that the substrate of the relativistic quantum field remains unchanged in the process of coupling the detector. The chosen combination has the additional advantage that the intraspecies scattering length of potassium is as small as $a_{aa} = 4 a_0$, which implies that an ensemble of impurities acts to a good approximation as independent particles. This is crucial for increasing the necessary statistics for protocols such as entanglement harvesting.

Entanglement harvesting from a BEC— When systems interact with a quantum field, there are two ways in which they can become entangled. The first (and most commonly considered) method is when the probes exchange information, and entanglement is mediated by the field. The second method for a field to entangle two probes is when the probes extract entanglement from the field itself, effectively performing an entanglement swap operation. These methods contribute differently in different regimes for the interaction between probes and field: in the long time limit, entanglement extraction is negligible compared to entanglement mediated through the field. On the other hand, in the short time limit, when the probes effectively cannot communicate, the only way they can become entangled is by extracting previously existing entanglement in the field (see Fig. 2). This can be used to infer the existence of entanglement between the

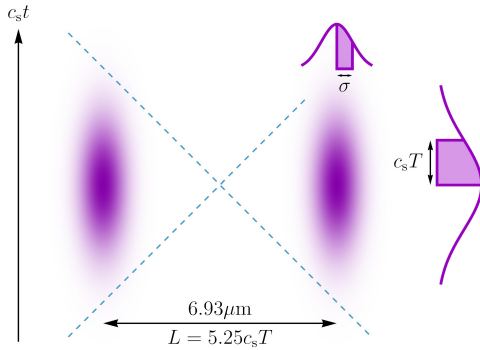


Figure 2. Spacetime density plot of the interaction regions $\Lambda_i(x) = \chi(t)f_i(\mathbf{x})$ for the probes. In the plot above we use $\sigma = 0.35c_s T$ for illustration purposes, corresponding to $\Omega/2\pi = 6$ kHz when using ^{39}K .

finite regions that the probes couple to, corresponding to the protocol of entanglement harvesting [31, 32, 34].

When two bound impurities (labelled A and B) initialized in their ground state interact with a BEC for finite times, their final state can be written as

$$\hat{\rho}_{AB} = \begin{pmatrix} 1 - \mathcal{L}_{AA} - \mathcal{L}_{BB} & 0 & 0 & \mathcal{M}^* \\ 0 & \mathcal{L}_{BB} & \mathcal{L}_{AB} & 0 \\ 0 & \mathcal{L}_{AB}^* & \mathcal{L}_{AA} & 0 \\ \mathcal{M} & 0 & 0 & 0 \end{pmatrix} + \mathcal{O}(g_{ab}^4), \quad (12)$$

where

$$\begin{aligned} \mathcal{L}_{IJ} &= \frac{\bar{g}_{ab}^2}{\hbar^2} \int d^4x d^4x' \Lambda_I(x) \Lambda_J(x') e^{-i\Omega(t-t')} \langle \delta\hat{\rho}(x) \delta\hat{\rho}(x') \rangle, \\ \mathcal{M} &= -\frac{\bar{g}_{ab}^2}{\hbar^2} \int d^4x d^4x' \Lambda_A(x) \Lambda_B(x') e^{i\Omega(t+t')} \langle \mathcal{T}(\delta\hat{\rho}(x) \delta\hat{\rho}(x')) \rangle, \end{aligned} \quad (13)$$

$I, J \in \{A, B\}$, $\Lambda_i(x) = \chi(t)f_i(\mathbf{x})$ are the spacetime smearing functions of the interactions, where $\chi(t)$ is determined by the time profile of the magnetic field applied to the system (Feshbach tuning) and $f_i(\mathbf{x})$ are determined by the trapping potentials. The entanglement in the final state of the probes can be quantified through the negativity [80], a faithful entanglement quantifier for systems of two qubits. Assuming identical shapes for the detectors, $\mathcal{L}_{AA} = \mathcal{L}_{BB} = \mathcal{L}$, the negativity can be written as

$$\mathcal{N} = \max(|\mathcal{M}| - \mathcal{L}, 0). \quad (14)$$

Overall, the negativity is a competition between a non-local term \mathcal{M} and local noise term \mathcal{L} , corresponding to the excitation probability of the detectors.

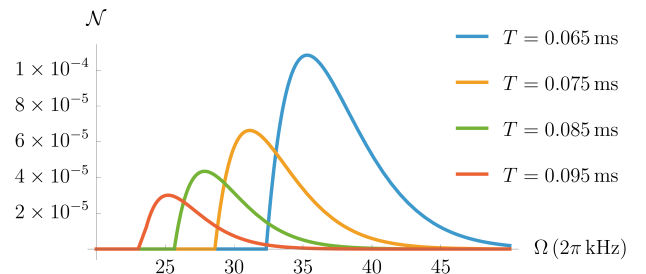


Figure 3. Negativity in the final state of the two impurities as a function of the trap frequency Ω for different values of interaction time parameter T .

Although the potential applications of entanglement harvesting range from entanglement quantification in quantum fields to relativistic quantum computing [81–85], the protocol is hindered by the notoriously small values of the extracted entanglement. However, the polaron detector model proposed here with ^{39}K coupled to a condensate of ^{87}Rb provides negativity values of the order of 10^{-4} even before any optimization of $\chi(t)$ and $f_i(\mathbf{x})$, being implementable with currently available methods.

In Fig. 3 we plot the negativity values (14) for the cho-

sen atomic species parameters as a function of the trapping frequency Ω for different values of the interaction time T . For analytical predictions we choose a Gaussian switching function $\chi(t) = e^{-t^2/2T^2}$ and approximated the spatial profile $f(\mathbf{x})$ by a normal distribution with standard deviation $\sigma = \sqrt{\hbar/m_a\Omega}$. In the plots we keep the probes separated by a distance $L = 5.25 c_s T$, of the order of $10\mu\text{m}$, ensuring that they can be placed within condensates of realizable sizes and minimal communication between the detectors. Indeed, in Appendix D we show that the signalling estimator [86] at the peak negativity values is negligible. The frequencies Ω corresponding to the negativity peaks are also within the regime where the rubidium condensate behaves relativistically (see Appendix D).

For detecting entanglement harvesting, the two observables \mathcal{L} and \mathcal{M} must be estimated from experimental data. While \mathcal{L} is directly accessible via the measured occupation of the excited state, extracting \mathcal{M} requires local control of the motional degree of freedom, i.e., a unitary rotation prior to detection. Coherent control of motional degrees of freedom has already been demonstrated and exploited in [65, 66]. The ultimate precision in estimating \mathcal{L} and \mathcal{M} is set by statistics due to the finite number of experimental repetitions. Since the expected negativity is on the order of 10% of the occupation number, achieving a relative statistical uncertainty of 10% requires at least $N \approx 100$ detection events, corresponding to $1/\sqrt{N} = 0.1$. Given an excitation probability of $\mathcal{L} \approx 10^{-3}$, this translates to more than 10^5 experimental realizations, which is well within reach of modern BEC experiments; for instance, a comparable number of repetitions was required for the first Fisher information estimation in BECs [87].

Conclusions—In this work we show that a bound im-

purity coupled to a BEC with controlled interspecies interaction is directly mapped onto the physics of a UDW detector interacting with a relativistic field. As a paradigmatic example of a relativistic quantum information protocol, we show that this implementation brings entanglement harvesting within experimental reach, even before any specific optimization.

Due to the pristine control over the spatial and temporal degrees of freedom, this BEC particle detector can be employed for probing local physics in relativistic scenarios not yet experimentally explored. This paves the way for implementations of protocols such as quantum collect calling [30] and quantum energy teleportation [28, 29, 88], that have their foundation on the underlying causal structure of spacetime.

Beyond controlling the probes, we can also envision pushing the relativistic field to theoretically challenging regimes, for instance by implementing self-interactions. The outcomes of these experiments can give an alternative input for tackling these problems, opening the doors to phenomenological approaches to relativistic quantum information.

ACKNOWLEDGMENTS

The authors thank Marcos Morote Balboa for verifying computations. We thank also Helmut Strobel, Brian Bostwick, Fabian Isler, and Alberto Sartori for scrutinizing the experimental parameters and experimental feasibility. TRP is thankful for financial support from the Olle Engkvist Foundation (no.225-0062). Nordita is partially supported by Nordforsk. This work was made possible by the Deutsche Forschungsgemeinschaft (DFG, German Research Foundation) under Germany’s Excellence Strategy EXC 2181/1 - 390900948 (the Heidelberg STRUCTURES Excellence Cluster).

[1] C. Viermann, M. Sparn, N. Liebster, M. Hans, E. Kath, A. Parra-Lopez, M. Tolosa-Simeon, N. Sanchez-Kuntz, T. Haas, H. Strobel, S. Floerchinger, and M. K. Oberthaler, Quantum field simulator for dynamics in curved spacetime, *Nature* **611**, 260 (2022).

[2] M. Tajik, M. Gluza, N. Sebe, P. Schüttelkopf, F. Cataldini, J. Sabino, F. Møller, S.-C. Ji, S. Erne, G. Guarneri, S. Sotiriadis, J. Eisert, and J. Schmiedmayer, Experimental observation of curved light-cones in a quantum field simulator, *Proceedings of the National Academy of Sciences* **120**, e2301287120 (2023).

[3] R. Schützhold, Ultra-cold atoms as quantum simulators for relativistic phenomena, *Progress in Particle and Nuclear Physics* **145**, 104198 (2025).

[4] C. F. Roos, R. Gerritsma, G. Kirchmair, F. Zähringer, E. Solano, and R. Blatt, Quantum simulation of relativistic quantum physics with trapped ions, *Journal of Physics: Conference Series* **264**, 012020 (2011).

[5] S. Longhi, Classical simulation of relativistic quantum mechanics in periodic optical structures, *Applied Physics B* **104**, 453 (2011).

[6] J. S. Pedernales, R. Di Candia, D. Ballester, and E. Solano, Quantum simulations of relativistic quantum physics in circuit qed, *New Journal of Physics* **15**, 055008 (2013).

[7] C. Barceló, S. Liberati, and M. Visser, Analogue gravity, *Living Reviews in Relativity* **14**, 3 (2011).

[8] Y. H. Shi, R. Q. Yang, Z. Xiang, *et al.*, Quantum simulation of hawking radiation and curved spacetime with a superconducting on-chip black hole, *Nature Communications* **14**, 3263 (2023).

[9] J. Steinhauer, M. Abuzarli, T. Aladjidi, T. Bienaimé, C. PiekarSKI, W. Liu, E. Giacobino, A. Bramati, and Q. Glorieux, Analogue cosmological particle creation in an ultracold quantum fluid of light, *Nature Commun.* **13**, 2890 (2022), arXiv:2102.08279 [cond-mat.quant-gas].

[10] Y. Deller, M. Gärttner, T. Haas, M. K. Oberthaler, M. Reh, and H. Strobel, Area laws and thermalization from classical entropies in a bose-einstein condensate, *Phys. Rev. A* **112**, L011303 (2025).

[11] V. Chandrasekaran, R. Longo, G. Penington, and E. Witten, An algebra of observables for de sitter space, *J. High*

Energy Phys. **2023** (2), 82.

[12] C. J. Fewster, D. W. Janssen, L. D. Loveridge, K. Rejzner, and J. Waldron, Quantum reference frames, measurement schemes and the type of local algebras in quantum field theory, Comm. in Math. Phys. **406**, 19 (2024).

[13] C. J. Fewster and R. Verch, Quantum Fields and Local Measurements, Commun. Math. Phys. **378**, 851 (2020).

[14] C. J. Fewster and R. Verch, Measurement in quantum field theory (2023), arXiv:2304.13356 [math-ph].

[15] E. Witten, Aps medal for exceptional achievement in research: Invited article on entanglement properties of quantum field theory, Rev. Mod. Phys. **90**, 045003 (2018).

[16] N. Klco, D. H. Beck, and M. J. Savage, Entanglement structures in quantum field theories: Negativity cores and bound entanglement in the vacuum, Phys. Rev. A **107**, 012415 (2023).

[17] N. Klco and D. H. Beck, Entanglement structures in quantum field theories. ii. distortions of vacuum correlations through the lens of local observers, Phys. Rev. A **108**, 012429 (2023).

[18] W. G. Unruh, Notes on black-hole evaporation, Phys. Rev. D **14**, 870 (1976).

[19] W. G. Unruh and R. M. Wald, What happens when an accelerating observer detects a Rindler particle, Phys. Rev. D **29**, 1047 (1984).

[20] B. DeWitt, *General Relativity; an Einstein Centenary Survey* (Cambridge University Press, Cambridge, UK, 1980).

[21] T. R. Perche, Localized nonrelativistic quantum systems in curved spacetimes: A general characterization of particle detector models, Phys. Rev. D **106**, 025018 (2022).

[22] T. R. Perche, J. Polo-Gómez, B. de S. L. Torres, and E. Martín-Martínez, Particle Detectors from Localized Quantum Field Theories (2023), arXiv:2308.11698 [quant-ph].

[23] S. Onoe, T. L. M. Guedes, A. S. Moskalenko, A. Leitensstorfer, G. Burkard, and T. C. Ralph, Realizing a rapidly switched unruh-dewitt detector through electro-optic sampling of the electromagnetic vacuum, Physical Review D **105**, 056023 (2022), arXiv:2103.14360 [quant-ph].

[24] F. F. Settembrini, F. Lindel, A. M. Herter, S. Y. Buhmann, and J. Faist, Detection of quantum-vacuum field correlations outside the light cone, Nature Communications **13**, 3383 (2022).

[25] A. Teixidó-Bonfill, X. Dai, A. Lupascu, and E. Martín-Martínez, Towards an experimental implementation of entanglement harvesting in superconducting circuits: effect of detector gap variation on entanglement harvesting (2025), arXiv:2505.01516 [quant-ph].

[26] C. Gooding, S. Biermann, S. Erne, J. Louko, W. G. Unruh, J. Schmiedmayer, and S. Weinfurtner, Interferometric unruh detectors for bose-einstein condensates, Physical Review Letters **125**, 213603 (2020), arXiv:2007.07160 [gr-qc].

[27] C. Gooding, A. Sachs, R. B. Mann, and S. Weinfurtner, Vacuum entanglement probes for ultra-cold atom systems, New Journal of Physics **26**, 105001 (2024).

[28] M. Hotta, Quantum measurement information as a key to energy extraction from local vacuums, Phys. Rev. D **78**, 045006 (2008).

[29] M. Hotta, Quantum Energy Teleportation: An Introductory Review (2011), arXiv:1101.3954 [quant-ph].

[30] R. H. Jonsson, E. Martín-Martínez, and A. Kempf, Information transmission without energy exchange, Phys. Rev. Lett. **114**, 110505 (2015).

[31] A. Valentini, Non-local correlations in quantum electrodynamics, Phys. Lett. A **153**, 321 (1991).

[32] B. Reznik, Entanglement from the vacuum, Foundations of Physics **33**, 167 (2003).

[33] B. Reznik, A. Retzker, and J. Silman, Violating Bell's inequalities in vacuum, Phys. Rev. A **71**, 042104 (2005).

[34] A. Pozas-Kerstjens and E. Martín-Martínez, Harvesting correlations from the quantum vacuum, Phys. Rev. D **92**, 064042 (2015).

[35] F. Grusdt, N. Mostaan, E. Demler, and L. A. Peña Ardila, Impurities and polarons in bosonic quantum gases: a review on recent progress, Reports on Progress in Physics **88**, 066401 (2025).

[36] P. Massignan, R. Schmidt, G. E. Astrakharchik, A. İmamoğlu, M. Zwierlein, J. J. Arlt, and G. M. Bruun, Polarons in atomic gases and two-dimensional semiconductors (2025), arXiv:2501.09618 [cond-mat.quant-gas].

[37] R. Haag, *Local Quantum Physics: Fields, Particles, Algebras* (Springer-Verlag Berlin Heidelberg, 1992).

[38] K. Fredenhagen, An Introduction to Algebraic Quantum Field Theory, in *Advances in algebraic quantum field theory*, edited by R. Brunetti, C. Dappiaggi, K. Fredenhagen, and J. Yngvason (2015) pp. 1–30.

[39] C. Fewster and K. Rejzner, Algebraic quantum field theory: An introduction, in *Progress and Visions in Quantum Theory in View of Gravity*, edited by F. Finster, D. Giulini, J. Kleiner, and J. Tolksdorf (Birkhäuser, 2020).

[40] T. R. Perche and E. Martín-Martínez, Role of quantum degrees of freedom of relativistic fields in quantum information protocols, Phys. Rev. A **107**, 042612 (2023).

[41] B. A. Juárez-Aubry and J. Louko, Onset and decay of the 1 + 1 Hawking-Unruh effect: what the derivative-coupling detector saw, Class. Quantum Gravity **31**, 245007 (2014).

[42] T. R. Perche and M. H. Zambianco, Duality between amplitude and derivative coupled particle detectors in the limit of large energy gaps, Phys. Rev. D **108**, 045017 (2023).

[43] A. Teixidó-Bonfill and E. Martín-Martínez, Derivative coupling enables genuine entanglement harvesting in causal communication, Phys. Rev. D **110**, 105016 (2024).

[44] E. Martín-Martínez, T. R. Perche, and B. de S. L. Torres, General relativistic quantum optics: Finite-size particle detector models in curved spacetimes, Phys. Rev. D **101**, 045017 (2020).

[45] S. W. Hawking, Particle creation by black holes, Comm. Math. Phys. **43**, 199 (1975).

[46] L. Hodgkinson, J. Louko, and A. C. Ottewill, Static detectors and circular-geodesic detectors on the Schwarzschild black hole, Phys. Rev. D **89**, 104002 (2014).

[47] J. Louko and D. Marolf, Inextendible Schwarzschild black hole with a single exterior: How thermal is the Hawking radiation?, Phys. Rev. D **58**, 024007 (1998).

[48] S. Takagi, Vacuum Noise and Stress Induced by Uniform Acceleration: Hawking-Unruh Effect in Rindler Manifold of Arbitrary Dimension, Prog. Theor. Phys. Supp. **88**, 1 (1986).

[49] L. C. B. Crispino, A. Higuchi, and G. E. A. Matsas, The Unruh effect and its applications, *Rev. Mod. Phys.* **80**, 787 (2008).

[50] J. Earman, The unruh effect for philosophers, *STUD HIST PHILOS M P* **42**, 81 (2011).

[51] T. R. Perche, General features of the thermalization of particle detectors and the Unruh effect, *Phys. Rev. D* **104**, 065001 (2021).

[52] A. Pozas-Kerstjens and E. Martín-Martínez, Entanglement harvesting from the electromagnetic vacuum with hydrogenlike atoms, *Phys. Rev. D* **94**, 064074 (2016).

[53] N. Funai, J. Louko, and E. Martín-Martínez, $\hat{p} \cdot \hat{A}$ vs $\hat{x} \cdot \hat{E}$: Gauge invariance in quantum optics and quantum field theory, *Phys. Rev. D* **99**, 065014 (2019).

[54] R. Lopp and E. Martín-Martínez, Quantum delocalization, gauge, and quantum optics: Light-matter interaction in relativistic quantum information, *Phys. Rev. A* **103**, 013703 (2021).

[55] R. Faure, T. R. Perche, and B. d. S. L. Torres, Particle detectors as witnesses for quantum gravity, *Phys. Rev. D* **101**, 125018 (2020).

[56] J. P. M. Pitelli and T. R. Perche, Angular momentum based graviton detector, *Phys. Rev. D* **104**, 065016 (2021).

[57] T. R. Perche, B. Ragula, and E. Martín-Martínez, Harvesting entanglement from the gravitational vacuum, *Phys. Rev. D* **108**, 085025 (2023).

[58] Notice that the finite coupling required by a detector of this type goes beyond probing finite pulses—it requires a finite time coupling even with the vacuum of the quantum field.

[59] W. G. Unruh, Experimental Black-Hole Evaporation?, *Phys. Rev. Lett.* **46**, 1351.

[60] L. J. Garay, J. R. Anglin, J. I. Cirac, and P. Zoller, Sonic analog of gravitational black holes in bose-einstein condensates, *Physical Review Letters* **85**, 4643 (2000).

[61] C. Barcelo, S. Liberati, and M. Visser, Analogue Gravity, *Living Rev. Relativ.* **8**, 12, gr-qc/0505065.

[62] L. P. Pitaevskii and S. Stringari, *Bose-Einstein Condensation and Superfluidity*, International Series of Monographs on Physics, Vol. 164 (Oxford University Press, Oxford, 2018) reprint.

[63] M. Tolosa-Simeón, Á. Parra-López, N. Sánchez-Kuntz, T. Haas, C. Viermann, M. Sparn, N. Liebster, M. Hans, E. Kath, H. Strobel, M. K. Oberthaler, and S. Floerchinger, Curved and expanding spacetime geometries in Bose-Einstein condensates, *Physical Review A* **106**, 033313 (2022), arXiv:2202.10441 [cond-mat.quant-gas].

[64] In the infinite volume limit, one has $1/V \sum_{\mathbf{k}} \rightarrow 1/(2\pi)^3 \int d^3 \mathbf{k}$.

[65] R. Scelle, T. Rentrop, A. Trautmann, T. Schuster, and M. K. Oberthaler, Motional coherence of fermions immersed in a bose gas, *Physical Review Letters* **111**, 070401 (2013), arXiv:1306.3308 [cond-mat.quant-gas].

[66] T. Rentrop, A. Trautmann, F. A. Olivares, F. Jendrzejewski, A. Komnik, and M. K. Oberthaler, Observation of the phononic lamb shift with a synthetic vacuum, *Phys. Rev. X* **6**, 041041 (2016).

[67] H. Fröhlich, Electrons in lattice fields, *Advances in Physics* **3**, 325 (1954).

[68] F. M. Cucchietti and E. Timmermans, Strong-Coupling Polarons in Dilute Gas Bose-Einstein Condensates, *Phys. Rev. Lett.* **96**, 210401.

[69] J. Tempere, W. Casteels, M. K. Oberthaler, S. Knoop, E. Timmermans, and J. T. Devreese, Feynman path-integral treatment of the BEC-impurity polaron, *Phys. Rev. B* **80**, 184504.

[70] C. Chin, R. Grimm, P. Julienne, and E. Tiesinga, Feshbach resonances in ultracold gases, *Rev. Mod. Phys.* **82**, 1225 (2010).

[71] first krb experiment, or general reference to mixtures, ()

[72] reference where the phonon field is defined as relativistic scalar quantum field, ()

[73] F. Schmidt, D. Mayer, M. Hohmann, T. Lausch, F. Kindermann, and A. Widera, Precision measurement of the ^{87}Rb tune-out wavelength in the hyperfine ground state $f = 1$ at 790 nm, *Phys. Rev. A* **93**, 022507 (2016).

[74] J. L. Ville, R. Saint-Jalm, É. Le Cerf, M. Aidelsburger, S. Nascimbène, J. Dalibard, and J. Beugnon, Sound propagation in a uniform superfluid two-dimensional Bose gas, *Phys. Rev. Lett.* **121**, 145301 (2018).

[75] E. W. Streed, S. Schabel, J. Mun, M. Boyd, G. K. Campbell, W. Ketterle, and D. E. Pritchard, Large atom number bose-einstein condensate machines, *Review of Scientific Instruments* **77**, 023106 (2006).

[76] F. Ferlaino, C. D'Errico, G. Roati, M. Zaccanti, M. Inguscio, G. Modugno, and A. Simoni, Feshbach spectroscopy of a K-Rb atomic mixture, *Phys. Rev. A* **73**, 040702 (2006).

[77] G. Thalhammer, G. Barontini, L. De Sarlo, J. Catani, F. Minardi, and M. Inguscio, Double species bose-einstein condensate with tunable interspecies interactions, *Phys. Rev. Lett.* **100**, 210402 (2008).

[78] L. Wacker, N. B. Jørgensen, D. Birkmose, R. Horchani, W. Ertmer, C. Klemp, N. Winter, J. Sherson, and J. J. Arlt, Tunable dual-species bose-einstein condensates of ^{39}K and ^{87}Rb , *Phys. Rev. A* **92**, 053602 (2015).

[79] L. J. Wacker, N. B. Jørgensen, D. Birkmose, N. Winter, M. Mikkelsen, J. Sherson, N. Zinner, and J. J. Arlt, Universal three-body physics in ultracold krb mixtures, *Phys. Rev. Lett.* **117**, 163201 (2016).

[80] G. Vidal and R. F. Werner, Computable measure of entanglement, *Phys. Rev. A* **65**, 032314 (2002).

[81] E. Martin-Martinez, D. Aasen, and A. Kempf, Processing quantum information with relativistic motion of atoms, *Phys. Rev. Lett.* **110**, 160501 (2013).

[82] D. E. Bruschi, A. Dragan, A. R. Lee, I. Fuentes, and J. Louko, Relativistic motion generates quantum gates and entanglement resonances, *Phys. Rev. Lett.* **111**, 090504 (2013).

[83] E. Martín-Martínez and C. Sutherland, Quantum gates via relativistic remote control, *Phys. Lett. B* **739**, 74–82 (2014).

[84] D. Layden, E. Martin-Martinez, and A. Kempf, Universal scheme for indirect quantum control, *Phys. Rev. A* **93**, 040301 (2016).

[85] P. A. LeMaitre, T. R. Perche, M. Krumm, and H. J. Briegel, Universal quantum computer from relativistic motion, *Phys. Rev. Lett.* **134**, 190601 (2025).

[86] E. Tjoa and E. Martín-Martinez, When entanglement harvesting is not really harvesting, *Phys. Rev. D* **104**, 125005 (2021).

[87] H. Strobel, W. Muessel, D. Linnemann, T. Zibold, D. B. Hume, L. Pezzé, A. Smerzi, and M. K. Oberthaler, Fisher information and entanglement of non-gaussian spin states, *Science* **345**, 424 (2014).

- [88] B. Ragula and E. Martín-Martínez, A review of applications of quantum energy teleportation: from experimental tests to thermodynamics and spacetime engineering (2025), arXiv:2505.04689 [quant-ph].
- [89] L. Pitaevskii and S. Stringari, *Bose-Einstein condensation and superfluidity*, Vol. 164 (Oxford University Press, 2016).
- [90] M. E. Peskin, *An Introduction to quantum field theory* (CRC press, 2018).
- [91] The signs are not the usual ones because the primary field (phase) is really the imaginary part of the original field (the linear fluctuations of the complex atomic field Ψ).
- [92] T. Lee and C. Yang, Many-body problem in quantum mechanics and quantum statistical mechanics, *Physical Review* **105**, 1119 (1957).
- [93] T. Lee and C. Yang, Low-temperature behavior of a dilute bose system of hard spheres. ii. nonequilibrium properties, *Physical Review* **113**, 1406 (1959).
- [94] T. R. Perche, Closed-form expressions for smeared bidistributions of a massless scalar field: Nonperturbative and asymptotic results in relativistic quantum information, *Phys. Rev. D* **110**, 025013 (2024).

Appendix A: Phonons as relativistic quantum fields

Here we show that the phase and density fluctuations of a uniform BEC are analogous to relativistic quantum fields in Minkowski spacetime. The (time-independent) field operator for the condensate is

$$\hat{\Psi}(\mathbf{x}) = \frac{1}{\sqrt{V}} \sum_{\mathbf{k}} \hat{a}_{\mathbf{k}} e^{i\mathbf{k}\cdot\mathbf{x}}$$

in a plane wave basis. Under the Bogoliubov approximation, we can split the field operator as

$$\hat{\Psi}(\mathbf{x}) = \Psi_0 + \delta\hat{\Psi}(\mathbf{x}) = \sqrt{\frac{N}{V}} + \frac{1}{\sqrt{V}} \sum_{\mathbf{k} \neq 0} a_{\mathbf{k}} e^{i\mathbf{k}\cdot\mathbf{x}}$$

where $\delta\hat{\Psi}(\mathbf{x})$ is the field operator of the fluctuations over the background. In the following, all the sums are meant excluding the $\mathbf{k} = 0$ component. In the Madelung representation $\Psi = \sqrt{\rho} e^{i\phi}$, expanding to first order fluctuations of the density and phase fields

$$\delta\hat{\Psi}(\mathbf{x}) = \frac{1}{2\sqrt{\rho_0}} \delta\hat{\rho}(\mathbf{x}) + i\sqrt{\rho_0} \delta\hat{\phi}(\mathbf{x}) \quad (\text{A1})$$

where $\rho_0 \equiv \Psi_0 = \sqrt{N/V}$ is the uniform background density of the condensate. Then

$$\begin{aligned} \delta\hat{\rho}(\mathbf{x}) &= \sqrt{\rho_0} \left(\delta\hat{\Psi} + \delta\hat{\Psi}^\dagger \right) = \sqrt{\frac{\rho_0}{V}} \sum_{\mathbf{k}} \left(\hat{a}_{\mathbf{k}} e^{i\mathbf{k}\cdot\mathbf{x}} + \hat{a}_{\mathbf{k}}^\dagger e^{-i\mathbf{k}\cdot\mathbf{x}} \right) \\ \delta\hat{\phi}(\mathbf{x}) &= \frac{1}{2i\sqrt{\rho_0}} \left(\delta\hat{\Psi} - \delta\hat{\Psi}^\dagger \right) = \frac{-i}{2\sqrt{\rho_0 V}} \sum_{\mathbf{k}} \left(\hat{a}_{\mathbf{k}} e^{i\mathbf{k}\cdot\mathbf{x}} - \hat{a}_{\mathbf{k}}^\dagger e^{-i\mathbf{k}\cdot\mathbf{x}} \right) \end{aligned}$$

Now we introduce phononic excitations by Bogoliubov transformations [89]. Let

$$\hat{a}_{\mathbf{k}} = u_{\mathbf{k}} \hat{b}_{\mathbf{k}} + v_{-\mathbf{k}}^* \hat{b}_{-\mathbf{k}}^\dagger, \quad \hat{a}_{\mathbf{k}}^\dagger = u_{\mathbf{k}}^* \hat{b}_{\mathbf{k}}^\dagger + v_{-\mathbf{k}} \hat{b}_{-\mathbf{k}}. \quad (\text{A2})$$

The density and fluctuations field take the form

$$\delta\hat{\rho}(\mathbf{x}) = \sqrt{\frac{\rho_0}{V}} \sum_{\mathbf{k}} \left\{ (u_{\mathbf{k}} + v_{\mathbf{k}}) \hat{b}_{\mathbf{k}} e^{i\mathbf{k}\cdot\mathbf{x}} + (u_{\mathbf{k}}^* + v_{\mathbf{k}}^*) \hat{b}_{\mathbf{k}}^\dagger e^{-i\mathbf{k}\cdot\mathbf{x}} \right\} \quad (\text{A3})$$

$$\delta\hat{\phi}(\mathbf{x}) = \frac{-i}{2\sqrt{\rho_0 V}} \sum_{\mathbf{k}} \left\{ (u_{\mathbf{k}} - v_{\mathbf{k}}) \hat{b}_{\mathbf{k}} e^{i\mathbf{k}\cdot\mathbf{x}} - (u_{\mathbf{k}}^* - v_{\mathbf{k}}^*) \hat{b}_{\mathbf{k}}^\dagger e^{-i\mathbf{k}\cdot\mathbf{x}} \right\}. \quad (\text{A4})$$

The $u_{\mathbf{k}}, v_{\mathbf{k}}$ coefficients can be chosen real as

$$u_{\mathbf{k}} = \sqrt{\frac{\hbar^2 |\mathbf{k}|^2 / 2m_b + g_{bb} \rho_0}{2\hbar\omega_{\mathbf{k}}} + \frac{1}{2}}, \quad v_{-\mathbf{k}} = -\sqrt{\frac{\hbar^2 |\mathbf{k}|^2 / 2m_b + g_{bb} \rho_0}{2\hbar\omega_{\mathbf{k}}} - \frac{1}{2}} \quad (\text{A5})$$

with Bogoliubov dispersion $\omega_{\mathbf{k}} = \sqrt{c_s^2 |\mathbf{k}|^2 + (\hbar^2 |\mathbf{k}|^2 / 2m_b)^2}$ and $c_s = \sqrt{g_{bb} \rho_0 / m_b}$. We are interested in the low energy limit $|\mathbf{k}| \ll m_b c_s / \hbar$, in which the phononic excitations can be considered as a relativistic quantum field. To see this, in this limit one finds

$$u_{\mathbf{k}} + v_{\mathbf{k}} \approx \sqrt{\frac{g_{bb} \rho_0}{2\hbar\omega_{\mathbf{k}}} + \frac{1}{2}} - \sqrt{\frac{g_{bb} \rho_0}{2\hbar\omega_{\mathbf{k}}} - \frac{1}{2}} \approx \sqrt{\frac{\hbar\omega_{\mathbf{k}}}{2g_{bb} \rho_0}}$$

$$u_{\mathbf{k}} - v_{\mathbf{k}} \approx \sqrt{\frac{g_{bb} \rho_0}{2\hbar\omega_{\mathbf{k}}} + \frac{1}{2}} + \sqrt{\frac{g_{bb} \rho_0}{2\hbar\omega_{\mathbf{k}}} - \frac{1}{2}} \approx 2\sqrt{\frac{g_{bb} \rho_0}{2\hbar\omega_{\mathbf{k}}}}.$$

Substitution in (A3) brings

$$\delta\hat{\rho}(\mathbf{x}) = \frac{1}{\sqrt{V}} \sum_{\mathbf{k}} \sqrt{\frac{\hbar\omega_{\mathbf{k}}}{2g_{bb}}} (\hat{b}_{\mathbf{k}} e^{i\mathbf{k}\cdot\mathbf{x}} + \hat{b}_{\mathbf{k}}^\dagger e^{-i\mathbf{k}\cdot\mathbf{x}}) \quad (\text{A6})$$

$$\delta\hat{\phi}(\mathbf{x}) = \frac{-i}{\sqrt{V}} \sum_{\mathbf{k}} \sqrt{\frac{g_{bb}}{2\hbar\omega_{\mathbf{k}}}} (\hat{b}_{\mathbf{k}} e^{i\mathbf{k}\cdot\mathbf{x}} - \hat{b}_{\mathbf{k}}^\dagger e^{-i\mathbf{k}\cdot\mathbf{x}}). \quad (\text{A7})$$

This shows that the quantum fluctuations of density and phase behave as massless relativistic quantum fields in the low energy regime, with dispersion (energy-momentum) relation $\omega_{\mathbf{k}} = c_s |\mathbf{k}|$, by straight comparison with the analogous expressions for a free massless scalar field in Minkowski spacetime [90]. The density field operator can be interpreted as the momentum conjugate to the phase field operator [91]. The classical Hamiltonian for the low energy theory is

$$H = \int d^n x \left\{ \frac{1}{2g_{bb}} (\delta\rho)^2 - \frac{\rho_0}{2m_b} (\partial_i \delta\phi)(\partial^i \delta\phi) \right\}. \quad (\text{A8})$$

It is straightforward to verify by substitution that the quantum Hamiltonian is

$$\hat{H} = \sum_{\mathbf{k}} \hbar\omega_{\mathbf{k}} \left(\hat{b}_{\mathbf{k}}^\dagger \hat{b}_{\mathbf{k}} + \frac{1}{2} \right) = \sum_{\mathbf{k}} \hbar\omega_{\mathbf{k}} \hat{b}_{\mathbf{k}}^\dagger \hat{b}_{\mathbf{k}} + E_0 \quad (\text{A9})$$

corresponding to the energy of free phonons plus zero-point energy. The apparently divergent zero-point energy is “renormalized” in this simple theory by going to higher order in the interaction expansion [92, 93]. We can turn the density and phase fluctuations field operators into time-dependent relativistic form by going from the Schrödinger to the Heisenberg picture. Using $e^{i\hat{H}t/\hbar} b_{\mathbf{k}} e^{-i\hat{H}t/\hbar} = b_{\mathbf{k}} e^{-i\omega_{\mathbf{k}}t}$ and its complex conjugate we obtain

$$\delta\hat{\rho}(\mathbf{x}) = \frac{1}{\sqrt{V}} \sum_{\mathbf{k}} \sqrt{\frac{\hbar\omega_{\mathbf{k}}}{2g_{bb}}} (\hat{b}_{\mathbf{k}} e^{i\mathbf{k}\cdot\mathbf{x}} + \hat{b}_{\mathbf{k}}^\dagger e^{-i\mathbf{k}\cdot\mathbf{x}}) \quad (\text{A10})$$

$$\delta\hat{\phi}(\mathbf{x}) = \frac{-i}{\sqrt{V}} \sum_{\mathbf{k}} \sqrt{\frac{g_{bb}}{2\hbar\omega_{\mathbf{k}}}} (\hat{b}_{\mathbf{k}} e^{i\mathbf{k}\cdot\mathbf{x}} - \hat{b}_{\mathbf{k}}^\dagger e^{-i\mathbf{k}\cdot\mathbf{x}}). \quad (\text{A11})$$

with $\mathbf{x} = (t, \mathbf{x})$ and $\mathbf{k} = (\omega_{\mathbf{k}}, \mathbf{k})$. The fields satisfy the usual equal-time commutation relations and

$$\hbar \frac{\partial}{\partial t} \delta\hat{\phi}(\mathbf{x}) = -g_{bb} \delta\hat{\rho}(\mathbf{x}) \quad (\text{A12})$$

which is the usual relation between density and phase fluctuations in a weakly interacting BEC.

Appendix B: Calculation of the excitation probability

The transition amplitude d between times t_i and t_f from the state $|g, 0\rangle$ (impurity in its ground state, no phonons) to the state $|e, \zeta\rangle$ (impurity in excited state, arbitrary number of phonons) for small coupling g_{IB} is given by first

order perturbation theory

$$d = \frac{i}{\hbar} \int_{t_i}^{t_f} dt \langle \zeta, e | \hat{H}_I(t) | g, 0 \rangle \quad (\text{B1})$$

where $\hat{H}_I(t)$, the interaction term in the Hamiltonian in the interaction picture, is

$$\hat{H}_I(t) = \int d^3x g_{ab}(t) \hat{\rho}_a(x) \hat{\rho}_b(x). \quad (\text{B2})$$

We write $\hat{\rho}_b(x) = \rho_0 + \delta\hat{\rho}(x)$, and drop the classical term ρ_0 . The impurity density operator in our setting becomes

$$\hat{\rho}_a(x) = f^*(x) e^{i\Omega t} \hat{\sigma}^+ + f(x) e^{-i\Omega t} \hat{\sigma}^- \quad (\text{B3})$$

with $f(x) = (\psi_g^* \psi_e)(x)$ in terms of the eigenfunction decomposition of the impurity. The excitation probability $|g\rangle \rightarrow |e\rangle$ is the sum over all possible states of the phonon field of the modulus of the transition amplitude squared. Let $|n_{\mathbf{k}}\rangle$ be a multi-phonon state in Fock space. We have

$$\begin{aligned} \mathcal{L} &= \sum_{n_{\mathbf{k}}} \left| -\frac{i}{\hbar} \int_{t_i}^{t_f} dt \langle n_{\mathbf{k}}, e | H_I(t) | g, 0 \rangle \right|^2 \\ &= \frac{1}{\hbar^2} \int_{t_i}^{t_f} \int_{t_i}^{t_f} dt dt' g_{IB}(t) g_{IB}(t') \\ &\quad \times \int d^3x \int d^3x' \langle g | \hat{\rho}_a(t', x') | e \rangle \langle e | \hat{\rho}_a(t, x) | g \rangle \times \sum_{n_{\mathbf{k}}} \langle 0 | \delta\hat{\rho}(t', x') | n_{\mathbf{k}} \rangle \langle n_{\mathbf{k}} | \delta\hat{\rho}(t, x) | 0 \rangle \\ &= \frac{1}{\hbar^2} \int_{t_i}^{t_f} \int_{t_i}^{t_f} dt dt' g_{IB}(t) g_{IB}(t') \int d^3x \int d^3x' f(x') f^*(x) \langle 0 | \delta\hat{\rho}(t', x') \delta\hat{\rho}(t, x) | 0 \rangle e^{i\Omega(t-t')} \\ &= \frac{\bar{g}_{ab}^2}{\hbar^2} \int_{t_i}^{t_f} \int_{t_i}^{t_f} dt dt' \int d^3x \int d^3x' \chi(t) f(x) \chi(t') f^*(x') \langle 0 | \delta\hat{\rho}(x) \delta\hat{\rho}(x') | 0 \rangle e^{-i\Omega(t-t')} \end{aligned}$$

using the properties of the ladder operators and the completeness relation $\mathbf{1} = \sum_{n_{\mathbf{k}}} |n_{\mathbf{k}}\rangle \langle n_{\mathbf{k}}|$. To get the last equality we wrote $g_{ab}(t) = \bar{g}_{ab}\chi(t)$ with $0 \leq \chi(t) \leq 1$ and performed a change of variables $x \leftrightarrow x'$. Notice that if $\chi(t)$ is only non-zero in a interval I contained in $[t_i, t_f]$, we can instead rewrite the integral as an integration over all of spacetime:

$$\mathcal{L} = \frac{\bar{g}_{ab}^2}{\hbar^2} \int d^4x d^4x' \Lambda(x) \Lambda^*(x') \langle 0 | \delta\hat{\rho}(x) \delta\hat{\rho}(x') | 0 \rangle e^{-i\Omega(t-t')} \quad (\text{B4})$$

$$= \frac{\bar{g}_{ab}^2}{\hbar^2} \left\langle \left(\int d^4x \Lambda(x) e^{-i\Omega t} \delta\hat{\rho}(x) \right) \left(\int d^4x' \Lambda^*(x') e^{i\Omega t'} \delta\hat{\rho}(x') \right) \right\rangle \quad (\text{B5})$$

$$= \frac{\bar{g}_{ab}^2}{\hbar^2} \langle \delta\hat{\rho}(\Lambda^-) \delta\hat{\rho}(\Lambda^+) \rangle, \quad (\text{B6})$$

where $\Lambda(x) = \chi(t)f(x)$ is the spacetime smearing function of the interaction.

Appendix C: Computing the \mathcal{L} and \mathcal{M} terms explicitly

In the continuum limit (infinite condensate volume), the two-point function of the Bose-Einstein condensate can be written as

$$\langle \delta\hat{\rho}(x) \delta\hat{\rho}(x') \rangle = \frac{1}{g_{bb}} \frac{1}{(2\pi)^3} \int d^3k \frac{\hbar\omega_k}{2} e^{ik \cdot (x-x')}, \quad (\text{C1})$$

where \mathbf{k} has units of inverse length, corresponding to the wavelengths of the density fluctuation field. We can then write the term \mathcal{L} as

$$\mathcal{L} = \frac{\bar{g}_{ab}^2}{\hbar^2} \int d^4x d^4x' \Lambda(x) \Lambda(x') e^{-i\Omega(t-t')} \langle \delta\hat{\rho}(x) \delta\hat{\rho}(x') \rangle \quad (C2)$$

$$= \frac{\bar{g}_{ab}^2}{g_{bb}\hbar} \frac{1}{(2\pi)^3} \int d^3k \frac{\omega_k}{2} \int d^4x d^4x' e^{-i\omega_k(t-t')} e^{i\mathbf{k}\cdot(\mathbf{x}-\mathbf{x}')} e^{-i\Omega(t-t')} \chi(t) \chi(t') f(\mathbf{x}) f(\mathbf{x}') \quad (C3)$$

$$= \frac{\bar{g}_{ab}^2}{g_{bb}\hbar} \frac{1}{(2\pi)^3} \int d^3k \frac{\omega_k}{2} |\tilde{\chi}(\omega_k + \Omega)|^2 \tilde{f}(-\mathbf{k}) \tilde{f}(\mathbf{k}), \quad (C4)$$

where

$$\tilde{\chi}(\omega) = \int dt \chi(t) e^{-i\omega t}, \quad (C5)$$

$$\tilde{f}(\mathbf{k}) = \int d^3x f(\mathbf{x}) e^{-i\mathbf{k}\cdot\mathbf{x}}, \quad (C6)$$

and we used that the switching function $\chi(t)$ is real. For convenience we define the coupling constant $\bar{\lambda}$

$$\bar{\lambda}^2 = \frac{\bar{g}_{ab}^2}{g_{bb}\hbar c_s}, \quad (C7)$$

use that $\omega_k \approx c_s |\mathbf{k}|$, and write the switching function as $\chi(t) = \beta(t/T)$, where β determines the profile of the interaction and T controls the interaction time. For instance, for a Gaussian pulse we have $\beta(t) = e^{-\frac{t^2}{2}}$ and T corresponds to its standard deviation. We then obtain $\tilde{\chi}(\omega) = T \tilde{\beta}(\omega T)$ and

$$\mathcal{L} = \bar{\lambda}^2 \frac{c_s^2 T^2}{(2\pi)^3} \int d^3k \frac{|\mathbf{k}|}{2} |\tilde{\beta}(T(c_s |\mathbf{k}| + \Omega))|^2 \tilde{f}(-\mathbf{k}) \tilde{f}(\mathbf{k}). \quad (C8)$$

We now define the rescaled time and frequencies $\bar{T} = c_s T$ and $\bar{\Omega} = \Omega/c_s$ (with units of length and inverse length, respectively), allowing us to recast

$$\mathcal{L} = \frac{\bar{\lambda}^2}{(2\pi)^3} \bar{T}^2 \int d^3k \frac{|\mathbf{k}|}{2} |\tilde{\beta}(\bar{T}(|\mathbf{k}| + \bar{\Omega}))|^2 \tilde{f}(-\mathbf{k}) \tilde{f}(\mathbf{k}). \quad (C9)$$

Importantly, the expression above with $\bar{\lambda} \mapsto \lambda/\sqrt{\hbar c}$, $\bar{T} \mapsto cT$, $\bar{\Omega} \mapsto \Omega/c$ corresponds to the excitation probability of a momentum-coupled UDW detector with switching function $\chi(t) = \beta(t/T)$.

Specializing to the case where $\beta(t) = e^{-\frac{t^2}{2}}$ and the smearing functions are

$$f(\mathbf{x}) = \frac{1}{(2\pi\sigma^2)^{\frac{3}{2}}} e^{-\frac{|\mathbf{x}|^2}{2\sigma^2}}, \quad (C10)$$

we can integrate \mathcal{L} in closed form:

$$\mathcal{L} = \frac{\bar{\lambda}^2}{(2\pi)^2} \bar{T}^2 \int d^3k \frac{|\mathbf{k}|}{2} |e^{-\bar{T}^2(|\mathbf{k}| + \bar{\Omega})^2} e^{-\sigma^2|\mathbf{k}|^2}| = \frac{\bar{\lambda}^2}{2\pi} \bar{T}^2 \int d|\mathbf{k}| |\mathbf{k}|^3 e^{-\bar{T}^2(|\mathbf{k}| + \bar{\Omega})^2} e^{-\sigma^2|\mathbf{k}|^2} \quad (C11)$$

$$= \frac{\bar{\lambda}^2 \bar{T}^2 e^{-\bar{T}^2 \bar{\Omega}^2} \left(2\sqrt{\sigma^2 + \bar{T}^2} (\sigma^2 + \bar{T}^4 \bar{\Omega}^2 + \bar{T}^2) - \sqrt{\pi} \bar{T}^2 \bar{\Omega} e^{\frac{\bar{T}^4 \bar{\Omega}^2}{\sigma^2 + \bar{T}^2}} (2\bar{T}^4 \bar{\Omega}^2 + 3(\sigma^2 + \bar{T}^2)) \operatorname{erfc}\left(\frac{\bar{T}^2 \bar{\Omega}}{\sqrt{\sigma^2 + \bar{T}^2}}\right) \right)}{8\pi (\sigma^2 + \bar{T}^2)^{7/2}} \quad (C12)$$

An analogous reasoning can be made for the \mathcal{M} term, although the computations are slightly more involved. Explicitly, we have

$$\mathcal{M} = -\frac{\bar{g}_{ab}^2}{\hbar^2} \int dV dV' \Lambda_A(x) \Lambda_B(x') e^{i\Omega(t+t')} \langle \mathcal{T}(\delta\hat{\rho}(x) \delta\hat{\rho}(x')) \rangle, \quad (C13)$$

$$= -\frac{\bar{g}_{ab}^2}{\hbar^2} \int dV dV' \Lambda_A(x) \Lambda_B(x') e^{i\Omega(t+t')} (\langle \delta\hat{\rho}(x) \delta\hat{\rho}(x') \rangle \theta(t-t') + \langle \delta\hat{\rho}(x') \delta\hat{\rho}(x) \rangle \theta(t'-t)), \quad (C14)$$

$$\begin{aligned}
&= -\frac{\bar{g}_{ab}^2}{g_{bb}\hbar(2\pi)^3} \int d^3\mathbf{k} \frac{\omega_{\mathbf{k}}}{2} \int d^4\mathbf{x} d^4\mathbf{x}' (e^{-i\omega_{\mathbf{k}}(t-t')} + i\mathbf{k}\cdot(\mathbf{x}-\mathbf{x}')) \theta(t-t') e^{i\Omega(t+t')} \chi(t) \chi(t') f(\mathbf{x}) f(\mathbf{x}' - \mathbf{L}) \\
&\quad + e^{i\omega_{\mathbf{k}}(t-t') - i\mathbf{k}\cdot(\mathbf{x}-\mathbf{x}')} \theta(t'-t) e^{i\Omega(t+t')} \chi(t) \chi(t') f(\mathbf{x}) f(\mathbf{x}' - \mathbf{L})) \\
&= -\frac{\bar{g}_{ab}^2}{g_{bb}\hbar(2\pi)^3} \int d^3\mathbf{k} \frac{\omega_{\mathbf{k}}}{2} \int dt dt' (e^{-i\omega_{\mathbf{k}}(t-t')} \theta(t-t') e^{-i\mathbf{k}\cdot\mathbf{L}} + e^{i\omega_{\mathbf{k}}(t-t')} \theta(t'-t) e^{i\mathbf{k}\cdot\mathbf{L}}) \chi(t) \chi(t') e^{i\Omega(t+t')} \tilde{f}(-\mathbf{k}) \tilde{f}(\mathbf{k}) \\
&= -\frac{\bar{g}_{ab}^2}{g_{bb}\hbar(2\pi)^3} \int d^3\mathbf{k} \frac{\omega_{\mathbf{k}}}{2} 2 \int dt dt' \chi(t) \chi(t') e^{i\Omega(t+t')} e^{-i\omega_{\mathbf{k}}(t-t')} \theta(t-t') e^{-i\mathbf{k}\cdot\mathbf{L}} \tilde{f}(-\mathbf{k}) \tilde{f}(\mathbf{k}),
\end{aligned} \tag{C15}$$

where in the last equality we made the changes of variables $t \leftrightarrow t'$ and $\mathbf{k} \mapsto -\mathbf{k}$ in the second summand. We now define

$$Q_{\chi}(\omega_{\mathbf{k}}, \Omega, T) = \int dt dt' \chi(t) \chi(t') e^{i\Omega(t+t')} e^{-i\omega_{\mathbf{k}}(t-t')} \theta(t-t'), \tag{C16}$$

and again assume that $\chi(t) = \beta(t/T)$ and $\omega_{\mathbf{k}} = c_s |\mathbf{k}|$, so that

$$Q_{\chi}(c_s |\mathbf{k}|, \Omega, T) = \int dt dt' \beta(t/T) \beta(t'/T) e^{i\Omega(t+t')} e^{-i c_s |\mathbf{k}|(t-t')} \theta(t-t') \tag{C17}$$

$$= T^2 \int du du' \beta(u) \beta(u') e^{i\Omega T(u+u')} e^{-i c_s T |\mathbf{k}|(u-u')} \theta(u-u') \tag{C18}$$

$$= T^2 Q_{\beta}(|\mathbf{k}|, \Omega, c_s T). \tag{C19}$$

Plugging this result into the expression for \mathcal{M} and using again $\bar{T} = c_s T$ and $\bar{\Omega} = \Omega/c_s$ yields

$$\mathcal{M} = -\bar{\lambda}^2 \frac{\bar{T}^2}{(2\pi)^3} \int d^3\mathbf{k} \frac{|\mathbf{k}|}{2} 2Q_{\beta}(|\mathbf{k}|, \bar{\Omega}, \bar{T}) e^{-i\mathbf{k}\cdot\mathbf{L}} \tilde{f}(-\mathbf{k}) \tilde{f}(\mathbf{k}). \tag{C20}$$

Once again, the expression above with $\bar{\lambda} \mapsto \lambda/\sqrt{\hbar c}$, $\bar{T} \mapsto cT$, $\bar{\Omega} \mapsto \Omega/c$ corresponds to the \mathcal{M} term of a momentum-coupled UDW detector with switching function $\chi(t) = \beta(t/T)$.

Specializing to the case where $\beta(t) = e^{-\frac{t^2}{2}}$ we find a closed-form expression for $Q(|\mathbf{k}|, \bar{\Omega}, \bar{T})$ [34, 57]:

$$2Q_{\beta}(|\mathbf{k}|, \bar{\Omega}, \bar{T}) = 2\pi e^{-(\bar{\Omega}^2 + |\mathbf{k}|^2)\bar{T}^2} (1 - i\text{erfi}(|\mathbf{k}|\bar{T})). \tag{C21}$$

Using the smearing functions as in Eq. (C10) we can write

$$\mathcal{M} = -\bar{\lambda}^2 \frac{\bar{T}^2}{(2\pi)^2} \int d^3\mathbf{k} \frac{|\mathbf{k}|}{2} e^{-(\bar{\Omega}^2 + |\mathbf{k}|^2)\bar{T}^2} (1 - i\text{erfi}(|\mathbf{k}|\bar{T})) e^{-i\mathbf{k}\cdot\mathbf{L}} e^{-\sigma^2 |\mathbf{k}|^2} \tag{C22}$$

$$= -\bar{\lambda}^2 \frac{\bar{T}^2}{2\pi} \int d|\mathbf{k}| d\theta \sin \theta \frac{|\mathbf{k}|^3}{2} e^{-(\bar{\Omega}^2 + |\mathbf{k}|^2)\bar{T}^2} (1 - i\text{erfi}(|\mathbf{k}|\bar{T})) e^{-i|\mathbf{k}||\mathbf{L}| \cos \theta} e^{-\sigma^2 |\mathbf{k}|^2} \tag{C23}$$

$$= -\bar{\lambda}^2 \frac{\bar{T}^2}{(2\pi)} \int d|\mathbf{k}| |\mathbf{k}|^3 e^{-(\bar{\Omega}^2 + |\mathbf{k}|^2)\bar{T}^2} (1 - i\text{erfi}(|\mathbf{k}|\bar{T})) \text{sinc}(|\mathbf{k}|L) e^{-\sigma^2 |\mathbf{k}|^2} \tag{C24}$$

$$= -\bar{\lambda}^2 \frac{\bar{T}^2}{2\pi |\mathbf{L}|} \int d|\mathbf{k}| |\mathbf{k}|^2 e^{-(\bar{\Omega}^2 + |\mathbf{k}|^2)\bar{T}^2} (1 - i\text{erfi}(|\mathbf{k}|\bar{T})) \text{sin}(|\mathbf{k}|L) e^{-\sigma^2 |\mathbf{k}|^2}. \tag{C25}$$

Although at first unhinged, the integral above can be computed in closed-form. First, define

$$\mathcal{M}^+ = -\bar{\lambda}^2 \frac{\bar{T}^2}{2\pi |\mathbf{L}|} \int d|\mathbf{k}| |\mathbf{k}|^2 e^{-(\bar{\Omega}^2 + |\mathbf{k}|^2)\bar{T}^2} \text{sin}(|\mathbf{k}|L) e^{-\sigma^2 |\mathbf{k}|^2} \tag{C26}$$

$$\mathcal{M}^- = i\bar{\lambda}^2 \frac{\bar{T}^2}{2\pi |\mathbf{L}|} \int d|\mathbf{k}| |\mathbf{k}|^2 e^{-(\bar{\Omega}^2 + |\mathbf{k}|^2)\bar{T}^2} \text{sin}(|\mathbf{k}|L) e^{-\sigma^2 |\mathbf{k}|^2} \text{erfi}(|\mathbf{k}|\bar{T}), \tag{C27}$$

so that $\mathcal{M} = \mathcal{M}^+ + \mathcal{M}^-$. The first integral involves only complex exponentials, Gaussians and polynomials and can

be solved using standard methods:

$$\mathcal{M}^+ = \frac{\bar{\lambda}^2 \bar{T}^2 e^{-\bar{T}^2 \bar{\Omega}^2} \left(\sqrt{\pi} e^{-\frac{L^2}{4(\sigma^2 + \bar{T}^2)}} (L^2 - 2(\sigma^2 + \bar{T}^2)) \operatorname{erfi} \left(\frac{L}{2\sqrt{\sigma^2 + \bar{T}^2}} \right) - 2L\sqrt{\sigma^2 + \bar{T}^2} \right)}{16\pi L (\sigma^2 + \bar{T}^2)^{5/2}}. \quad (\text{C28})$$

The integral defining \mathcal{M}^- is less trivial. To solve it we first state the result shown in [94]:

$$\int d|\mathbf{k}| e^{-(\bar{T}^2 + \sigma^2)|\mathbf{k}|^2} \sin(|\mathbf{k}|L) \operatorname{erfi}(|\mathbf{k}|\bar{T}) = \frac{e^{-\frac{L^2}{4(\bar{T}^2 + \sigma^2)}}}{\sqrt{\bar{T}^2 + \sigma^2}} \frac{\sqrt{\pi}}{2} \operatorname{erf} \left(\frac{L\bar{T}}{2\sqrt{\sigma^2}\sqrt{\bar{T}^2 + \sigma^2}} \right). \quad (\text{C29})$$

We can now recast the integral of \mathcal{M}^- as

$$\mathcal{M}^- = i\bar{\lambda}^2 \frac{\bar{T}^2 e^{-\bar{\Omega}^2 \bar{T}^2}}{2\pi |\mathbf{L}|} \int d|\mathbf{k}| |\mathbf{k}|^2 e^{-(\bar{T}^2 + \sigma^2)|\mathbf{k}|^2} \sin(|\mathbf{k}|L) \operatorname{erfi}(|\mathbf{k}|\bar{T}) \quad (\text{C30})$$

$$= i\bar{\lambda}^2 \frac{\bar{T}^2 e^{-\bar{\Omega}^2 \bar{T}^2}}{2\pi |\mathbf{L}|} \int d|\mathbf{k}| \left(-\frac{d}{d\sigma^2} e^{-(\bar{T}^2 + \sigma^2)|\mathbf{k}|^2} \right) \sin(|\mathbf{k}|L) \operatorname{erfi}(|\mathbf{k}|\bar{T}) \quad (\text{C31})$$

$$= i\bar{\lambda}^2 \frac{\bar{T}^2 e^{-\bar{\Omega}^2 \bar{T}^2}}{2\pi |\mathbf{L}|} \left(-\frac{d}{d\sigma^2} \left(\int d|\mathbf{k}| e^{-(\bar{T}^2 + \sigma^2)|\mathbf{k}|^2} \sin(|\mathbf{k}|L) \operatorname{erfi}(|\mathbf{k}|\bar{T}) \right) \right) \quad (\text{C32})$$

$$= i\bar{\lambda}^2 \frac{\bar{T}^2 e^{-\bar{\Omega}^2 \bar{T}^2}}{2\pi |\mathbf{L}|} \left(-\frac{d}{d\sigma^2} \left(\frac{e^{-\frac{L^2}{4(\bar{T}^2 + \sigma^2)}}}{\sqrt{\bar{T}^2 + \sigma^2}} \frac{\sqrt{\pi}}{2} \operatorname{erf} \left(\frac{L\bar{T}}{2\sqrt{\sigma^2}\sqrt{\bar{T}^2 + \sigma^2}} \right) \right) \right). \quad (\text{C33})$$

The operation above then gives us

$$\mathcal{M}^- = -\frac{i\bar{\lambda}^2 \bar{T}^2 e^{-\bar{T}^2 \bar{\Omega}^2 - \frac{L^2}{4\sigma^2}} \left(\sqrt{\pi} \sigma^3 e^{\frac{L^2 \bar{T}^2}{4\sigma^2(\sigma^2 + \bar{T}^2)}} (L^2 - 2(\sigma^2 + \bar{T}^2)) \operatorname{erf} \left(\frac{L\bar{T}}{2\sigma\sqrt{\sigma^2 + \bar{T}^2}} \right) - 2L\bar{T}\sqrt{\sigma^2 + \bar{T}^2} (2\sigma^2 + \bar{T}^2) \right)}{16\pi L \sigma^3 (\sigma^2 + \bar{T}^2)^{5/2}}. \quad (\text{C34})$$

Appendix D: Signalling between the probes and relativistic behaviour

We can quantify how much of the entanglement between the probes is due to signaling by using the signaling estimator defined in [86]:

$$\mathcal{I} = \begin{cases} \frac{\mathcal{N}^-}{\mathcal{N}} & \mathcal{N} > 0 \\ 0 & \mathcal{N} = 0, \end{cases} \quad (\text{D1})$$

where $\mathcal{N}^- = \max(0, |\mathcal{M}^-| - \mathcal{L})$, where \mathcal{M}^- corresponds to the causal exchanges encoded in the \mathcal{M} term, and is defined in Section C. This estimator satisfies $0 \leq \mathcal{I} \leq 1$ such that $\mathcal{I} = 0$ implies that the entanglement comes entirely from quantum fluctuations of the field (encoded in the term \mathcal{M}^+), and $\mathcal{I} = 1$ corresponds to the case where all entanglement acquired by the probes is due to communication through the field.

In Figure 4 we plot the signaling estimator as a function of the frequency of the trapping potential Ω for the setups considered in Figure 2 of the main text, when two potassium probes couple to a rubidium condensate for times of the order of ms while separated by distances $L = 5.25c_s T$, of the order of μm . In the setups considered, the signaling estimator stays below 30%. Moreover, at the peak negativity values displayed in the main text we have \mathcal{I} identically zero, implying that these cases correspond to genuine entanglement harvesting, where communication between the probes is negligible.

The density fluctuations behave relativistically for wavenumbers with $|\mathbf{k}| \leq \xi^{-1}$, where ξ is the healing length. We can estimate the wavenumbers relevant in the protocol of entanglement harvesting by writing the relevant terms \mathcal{L} ,

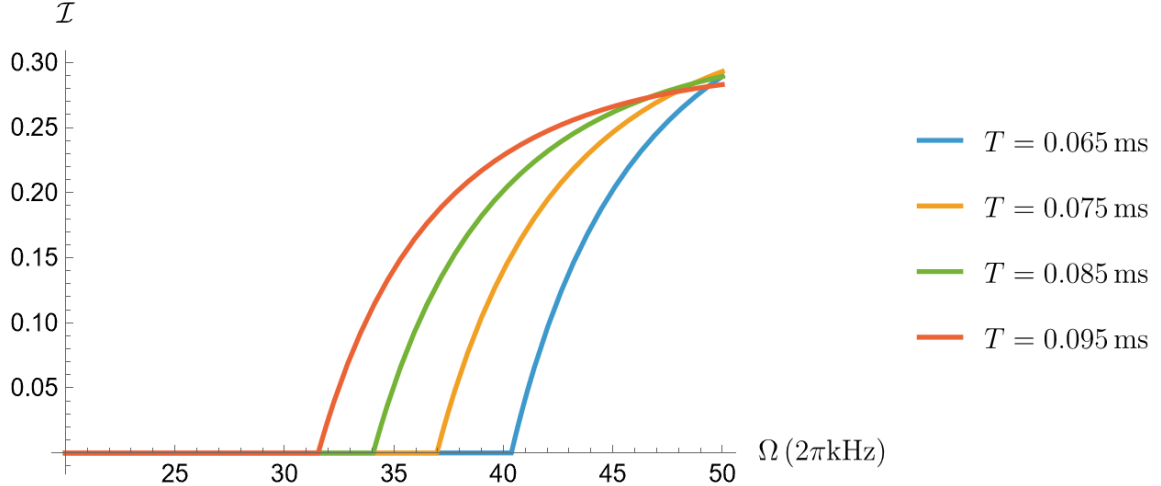


Figure 4. Plot of the signaling estimator as a function of Ω for the different setups considered in Fig. 2 of the main text when potassium probes coupled to a rubidium BEC are separated by distances $L = 5.25c_s T$.

\mathcal{M}^+ and \mathcal{M}^- as an integral in $|\mathbf{k}|$:

$$\mathcal{L} = \int d|\mathbf{k}| \mathcal{L}(|\mathbf{k}|) \quad (D2)$$

$$\mathcal{M}^+ = \int d|\mathbf{k}| \mathcal{M}^+ (|\mathbf{k}|) \quad (D3)$$

$$\mathcal{M}^- = \int d|\mathbf{k}| \mathcal{M}^- (|\mathbf{k}|). \quad (D4)$$

We plot these functions as a function of $|\mathbf{k}|$ for the protocol utilizing potassium impurities coupled to a rubidium BEC ($\xi = 120$ nm) in Fig. 5 when the interaction times are controlled by the parameter $T = 0.065$ ms, the probes are separated by $L = 5.25c_s T$ and the frequency of the harmonic traps correspond to the negativity peak $\Omega = 35 \times 2\pi$ kHz. We see that the relevant terms for genuine entanglement harvesting, $\mathcal{L}(|\mathbf{k}|)$ and $\mathcal{M}^+ (|\mathbf{k}|)$ are well within the relativistic regime, with the integrands only being relevant for frequencies smaller than the healing length. Although the tails of $\mathcal{M}^- (|\mathbf{k}|)$ extend up to 6 (nm)^{-1} , less than 7% of its total integral is contained in the region $|\mathbf{k}| > \xi^{-1}$.

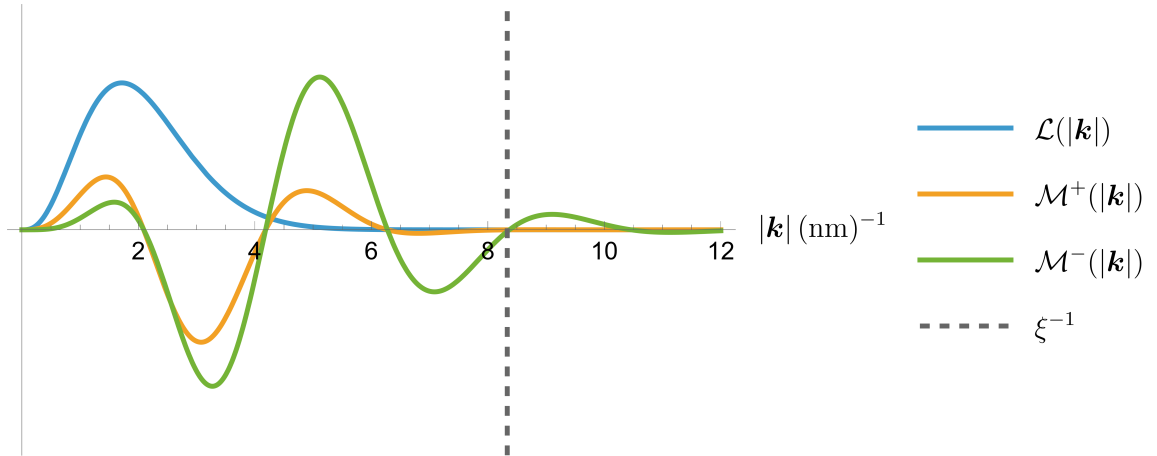


Figure 5. Plot of the integrands $\mathcal{L}(|\mathbf{k}|)$, $\mathcal{M}^+ (|\mathbf{k}|)$, and $\mathcal{M}^- (|\mathbf{k}|)$ as a function of $|\mathbf{k}|$ for two potassium impurities probing a rubidium BEC while separated by a distance $L = 5.25c_s T$, where $T = 0.065$ ms controls the time profile of the interaction, and the trap frequency of the impurities is $\Omega = 35 \times 2\pi$ kHz